

Co-solvent and temperature effect on conformation and hydration of polypropylene and polyethylene oxides in aqueous solutions

Rasika Dahanayake, Udaya Dahal, Elena E. Dormidontova*

Polymer Program, Institute of Materials Science and Physics Department, University of Connecticut, Storrs, Connecticut, 06269

Abstract

Understanding the origin of conformational changes of water-soluble polymers, as affected by external triggers such as temperature or co-solvent addition, is important from a fundamental perspective and for practical applications in responsive materials. Using atomistic molecular dynamics simulations we investigate conformational changes of polypropylene oxide (PPO) in connection to its hydration and capability to form hydrogen bonds upon either a temperature change or addition of another protic solvent (isobutyric acid, IBA) to aqueous solution. We demonstrate that upon addition of a very small amount of IBA, PPO starts to lose hydrogen bonds with water and form stable IBA-PEO hydrogen bonds, which act as a nucleation site for polymer collapse. With further addition of IBA, PPO resides at the IBA/water interface to retain some fraction of hydrogen bonds with water along with IBA-water hydrogen bonds. Unlike PEO where water mostly forms doubly-bonded hydrogen bonds (both hydrogens take part in h-bonding), PPO is hydrated by singly bonded water molecules in its hydration shell. As temperature increases breaking one of the hydrogen bonds in water doubly-bonded with PEO results in singly-bonded water. As a result, PEO retains water in its hydration shell even with a temperature increase and does not collapse upon temperature increase or IBA addition. Furthermore, PEO is capable of maintaining 80% of its hydrogen bonding with water even when it resides in an IBA-rich phase, while PPO retains less than 40% of hydrogen bonds with water while residing at the IBA/water interface. These results illustrate that hydrogen bonding and a polymer's capability to maintain its hydration shell are the key factors in polymer responsiveness to external triggers, factors that should be taken into consideration upon responsive material design and applications.

Keywords: polypropylene oxide, hydrogen bonding, coil-globule transition, co-solvent/water solution, molecular dynamics simulations, polyethylene oxide

1. Introduction

Water-soluble responsive polymers are actively used in many nanotechnological applications including biomedical applications [1–5]. In many applications it is essential to be able to control the polymer conformation in solution in different environments. Therefore a fundamental understanding of the mechanism and triggers for the conformational change of macromolecules is required for designing and functioning of responsive materials. There has been considerable experimental and theoretical interest in studying co-solvent effects on macromolecular conformation in solution [6,7,16–23,8–15]. A large class of polymers, such as polyethylene oxide (PEO), polypropylene oxide (PPO), poly(N-isopropylacrylamide) (PNIPAAm), polyvinylpyrrolidone (PVP), polyvinyl alcohol(PVA), etc. rely on hydrogen bonding with water for their solubility. Thus multiple triggers such as temperature and co-solvents that affect polymer-water hydrogen bonding can lead to significant conformational changes. [11,14,20,23,24] For this class of polymers the balance between hydrophobic/hydrophilic (excluded volume) interactions and hydrogen bonding is especially delicate and hard to interrogate experimentally or by using coarse-grained simulations. Atomistic molecular dynamics simulations are best suited for studying polymer hydration and interactions between polymer and solvents. In this paper using atomistic molecular dynamics simulations we investigate the effect of temperature and co-solvent on hydrogen bonding, polymer hydration and conformation for polypropylene oxide (PPO) in comparison with that for polyethylene oxide (PEO) and identify the mechanism for the observed conformational changes, which is the key for understanding the properties of this class of polymers in mixed solvents.

Experimental research on co-solvent effects on the conformational behavior of water-soluble polymers has been mostly centered around poly(N-isopropylacrylamide) (PNIPAAm) [6,21,25] and poly(N-diethyl acrylamide) (PDEA) [20]. Using microcalorimetry Tirrell *et al* [21] have observed that at low concentration PNIPAAm undergoes a coil-globule-coil conformational transformation in water-methanol mixed solvent. The data suggest that alcohol reduces the number or strength of the polymer-water contacts. Similar results have been observed also in water-dioxane and water-tetrahydrofuran (THF) mixed solvents. Hammouda *et al* investigated coil-globule-coil conformational change of PNIPAAm in water-ethanol mixed solvents.[8] They observe that PNIPAM was soluble and exhibited LCST behavior when the water content was 0-40% and 80-100% in the mixed solvent but collapsed in the intermediate region with water content 50-70%. The results of the above-mentioned experiments were rationalized within the Flory-Huggins ternary solution model with excluded volume interactions [8]. Wu *et al* have also investigated experimentally the coil-globule-coil conformational transformation of PNIPAAm in water/methanol mixed solvent [6]. It was observed that PNIPAAm was in a coil state until the methanol molar fraction reached 0.17 after which it transitioned into a globule state, which was stable in the range of methanol mole fraction 0.17-0.40 and then returned to a coil state at a higher methanol content. They proposed that the observed conformational changes of PNIPAAm are due to formation of water/methanol complexes, which represent a poor solvent for PNIPAAm. A different theoretical explanation for these experimental data was suggested by Winnik *et al* who used a co-hydration model,[25] accounting for the competitive hydrogen bond

formation between polymer-water and polymer-methanol in solution. The theoretical model proposed by Kremer *et al* considers conformational changes for a generic polymer in a mixture of good solvents and explains the reentrant conformational transition by the preferential coordination with one of the solvents.[9][10] The united atom OPLS simulations by Kremer *et al* specify the coordination mechanism for methanol in PNIPAAm aqueous solutions: PNIPAAm collapse occurs due to methanol bridging between NIPAAm monomers thereby reducing the hydrogen bonds between the polymer and water. A similar mechanism was suggested for PNIPAAm collapse in urea-water mixed solvent [11,12]. Dudowicz *et al* [22] and Schild *et al* [21] argued that co-solvent induced coil-globular-coil conformational changes of polymers can be well described (at least at higher polymer concentrations) within the Flory-Huggins three component model without involvement of the intramolecular bridging of NIPAAm by co-solvent. The coarse grained simulations by Der Vegt *et al* also demonstrate that excluded volume interactions alone can drive coil-globule-coil transition of PNIPAAm.[17–19]. They show that amphiphilic co-solvents, such as alcohols, can reduce the interfacial free energy of the polymer-cosolvent interactions by adsorbing on the polymer similar to a surfactant-like mechanism [17–19].

There is an obvious active interest in understanding the origin of solvent-induced conformational changes. The molecular details of the co-solvent interactions with macromolecules are difficult to ascertain from experimental data or coarse-grained computer simulations. Atomistic molecular dynamics simulations, where we can study hydrogen bonding explicitly, can provide such information. To date there have been only a few studies of this type. Using atomistic molecular dynamics simulations with the OPLS-AA forcefield Odriozola *et al* have recently modeled the coil-globule transition of PNIPAAm in water-acetone [13] and propanol-water mixed solvents [14]. They found that acetone absorbs on the methyl groups thereby blocking water from forming hydrogen bonds with amide groups, while propanol molecules can form bridges between PNIPAAm monomers and reduce the number of hydrogen bonds with water, leading in both cases to polymer collapse. As the co-solvent concentration increases it accumulates in the vicinity of PNIPAAm which causes the polymer to expand.

Formation of intramolecular crosslinks or bridges by co-solvent is proposed as one of the possible mechanisms of PNIPAAm collapse, so it is informative to compare its behavior to other water-soluble polymers, such as PPO, PEO [26] and polyvinylpyrrolidone (PVP) [27,28] that cannot form intramolecular hydrogen bonds. Experimentally Guettari *et al* observed the coil-globule-coil transition of PVP upon addition of ethanol to aqueous solutions [19]. The transition was attributed to the change of solvent quality due to formation of water-ethanol hydrogen bonding. These results indicate that co-solvent induced conformational transformations do not necessarily rely on intramolecular bonding. Experimental results by Greer *et al* showed that the coil conformation of PEO in water changes into a helical one in the presence of a large amount of isobutyric acid (IBA) [29]. Atomistic molecular dynamics simulations by some of us [30] reproduced the experimentally observed conformational transformation of PEO from coil to helix upon IBA addition to aqueous solution and demonstrated that the helical conformation of PEO is stabilized by long-lived IBA-PEO hydrogen bonds. While PEO is well-hydrated due to extensive hydrogen bonds with water [30–32] and remains soluble until very high temperatures, PPO is more hydrophobic, forms fewer hydrogen bonds with water and loses its solubility at low

temperature, similar to PNIPAAm (at least for relatively low molecular weights of PPO), [24,33]. Thus, it is informative to compare the effect of co-solvent on the conformational behavior of PPO in comparison to the reported PEO and PNIPAAm behavior. We are not aware of any experimental or theoretical/computational work on PPO behavior in mixed solvents. MD simulations by Roccatano *et al.* showed that the conformation of PPO (and PEO) and hydrogen bonding varies in different pure solvents [26]. Thus, one can also expect differences in preferential solvation when a polymer is exposed to a mixed solvent. In this manuscript, using atomistic MD simulations with the OPLS-AA force field and our modified PPO model, which reproduces the experimentally observed temperature induced coil-globule transition of PPO in aqueous solution, [33], we investigate changes in PPO conformation and hydration as a function of IBA concentration in mixed water/IBA solvent. We compare the co-solvent effect on PPO and PEO conformation and make conclusions on the similarities and differences of polymer behavior based on their ability to form hydrogen bonds with water and IBA and the overall co-solvent affinity for the polymer. Furthermore, we analyze the molecular mechanism of the coil-globule-coil conformational transformation of PPO upon co-solvent addition and discuss the importance of polymer hydration in the prediction of polymer behavior affected by temperature or co-solvent. We believe these insights can be applied to help understand the complex behaviors exhibited by responsive polymer materials in various applications.

2. Computational Details

To investigate temperature-induced conformational changes of polypropylene oxide (PPO) in aqueous solutions, we performed atomistic molecular dynamics simulations of PPO of two molecular weights $M_w = 4000 \text{ g/mol}$ ($N=69$) and $M_w = 2000 \text{ g/mol}$ ($N=35$) as well as for $M_w = 1000 \text{ g/mol}$ ($N=16$). The simulations were performed using the GPU-enabled version of GROMACS 4.6.5 with SPC/E water model [34,35] using the OPLS force-field [36]. SPC/E water model is one of the commonly used 3-point model of water, which reproduces rather well essential water properties [37–39]. It has been previously successfully employed by some of us to study PEO conformation in aqueous solutions and as part of self-assembled structures [30,40,41]. The existing models for PPO [26,42–46], including the OPLS force-field [36] do not reproduce experimentally observed conformational changes of PPO with an increase in temperature [24,47,48], as shown in Supplementary material (Table S1) thus we modified the OPLS force field accordingly, while keeping LJ interactions and 0.06e charge for hydrogens. We slightly modified the partial charges of PPO, as shown in Supplementary material (Scheme S1 and Table S2) and adopted the dihedrals suggested by Bedrov [44] and Roccatano [45], as shown in Table S3 of Supplementary material. With these modifications we were able to observe the coil-globular transition for the PPO chains of different lengths studied at the temperature range consistent with experimental observations [24,47,48].

The simulations were performed with NPT ensemble with a pressure of 1 bar in a $9 \times 9 \times 9 \text{ nm}^3$ periodic box. The number of water molecules in simulation box are listed in Supplementary material (Table S4). For PPO-2000 ($M_w = 2000 \text{ g/mol}$) we varied temperature from 7 °C to 50 °C, while for the PPO-4000 ($M_w = 4000 \text{ g/mol}$) temperature ranged from 2 °C to 22 °C. The temperature coupling was done using the v-rescale thermostat with coupling constant of 1 ps.

Pressure coupling was carried out using Berendsen barostat for the initial 30 ns of equilibration time. Then the production run was continued with the Parinello-Rahman barostat for 600 ns to 800 ns with a coupling constant of 1 ps. The integration time step for simulations were 2 fs. Electrostatic interactions were calculated using PME (Particle-Mesh Ewald) summation. A long range dispersion correction was applied for energy and pressure.

To study the co-solvent effect simulations were performed for a single PPO chain of $M_w = 4000 \text{ g/mol}$ (n=67) in water and isobutyric acid mixed solvent in a $9 \times 9 \times 9 \text{ nm}^3$ periodic box. For isobutyric acid we used the standard OPLS force field [36], as it was employed in one of our previous publications [30]. The MD simulation settings for the co-solvent simulation were identical to the temperature dependence simulations, except all simulations were performed at a constant temperature of 11 °C with IBA volume fraction for mixed solvent ranging between 0 and 1.

In our simulations the hydrogen bonds were characterized using a geometrical criteria: donor-acceptor distance (r_{DA}) $\leq 3.5 \text{ \AA}$ and hydrogen-donor-acceptor angle $\leq 30^\circ$ [30,49,50]. To further analyze the hydration properties of PPO the hydration shell was calculated using the geometrical distance criterion for the polymer backbone (i.e. all atoms but hydrogens) to water oxygen distance of $r_{\text{shell}} \leq 3.5 \text{ \AA}$.

To characterize the coil globule transition of PPO molecule, we analyzed the radius of gyration (R_g). The radius of gyration (equation 1) can be obtained from the principal moments (eigen values) of the gyration tensor as;

$$R_g = \sqrt{\lambda_1^2 + \lambda_2^2 + \lambda_3^2} \quad (1)$$

where $\lambda_1 > \lambda_2 > \lambda_3$.

To further understand the dynamics of IBA and water molecules hydrogen bonded to PPO the residence time correlation $C(t)$ for solvent remaining hydrogen bonded to PPO at time t is calculated. We marked the solvent molecules hydrogen bonded to PPO at time $t_0 = 0$ and calculated the following function:

$$C(t) = \langle \frac{N_s(t)}{N_s(t_0)} \rangle \quad (2)$$

where $N_s(t_0)$ is the number of IBA or water molecules hydrogen bonded to water at time $t_0 = 0$ and $N_s(t)$ is the number of the original IBA or water molecules that are still hydrogen bonded to the PPO molecule at time t . When calculating the number of water molecules we considered the total number of hydrogen bonded molecules regardless of whether they are singly or doubly bonded to PPO.

The visualization of the simulations results was performed using Visual Molecular Dynamics (VMD) [51].

3. Results and Discussion

We performed a set of atomistic molecular dynamics simulations at different temperatures and investigated PPO conformation and hydration in aqueous solution. In agreement with experimental data [24,48], we observed that at low temperature PPO assumes an expanded coil conformation, while with an increase in temperature the polymer conformation becomes more compact and above a certain temperature PPO collapses into a globule. Starting from a collapsed conformation obtained at high temperature and subsequently decreasing the temperature results in an expanded polymer conformation (Figure S1 of Supplementary material).

We analyzed the statistical occurrence of different conformations over time at a given temperature. Typical trajectories are shown in Figure S2 of Supplementary material. Figure 1 shows the distributions for the radius of gyration, R_g , of PPO-4000 averaged over the last 550 ns of simulation trajectories at different temperatures in the range between 2°C to 22°C. As is seen, at low temperature the distribution of R_g is rather broad with a maximum occurring at about 1.7nm, indicating that the molecule is well-solubilized in water and explores a range of expanded conformations with anisotropy being consistent with a coil conformation (Figure S3 of Supplementary material). As the temperature increases, the distribution becomes somewhat narrower and at 11°C and 12°C an additional peak at about 1.1-1.2nm starts to appear. As the temperature increases further, only a collapsed state with $R_g \approx 1.1\text{nm}$ can be observed. Correspondingly, the anisotropy parameter decreases to 0.2 (Figure S3 of Supplementary material) indicating a spherically symmetric globule. The corresponding Gaussian distribution is rather narrow indicating a strong preference for the collapsed state at elevated temperatures. Comparing distributions at low and high temperatures one can notice that in the transition temperature range the R_g distribution is bimodal with two peaks, one corresponding to an expanded state, similar to what is seen at lower temperature, and one to a collapsed state, as is dominate at high temperatures. The bimodal distribution indicates that the molecule explores both states spending about 70% of the time in an expanded state and 30% in the collapsed state (as is seen from trajectories in Supplementary material, Figure S2).

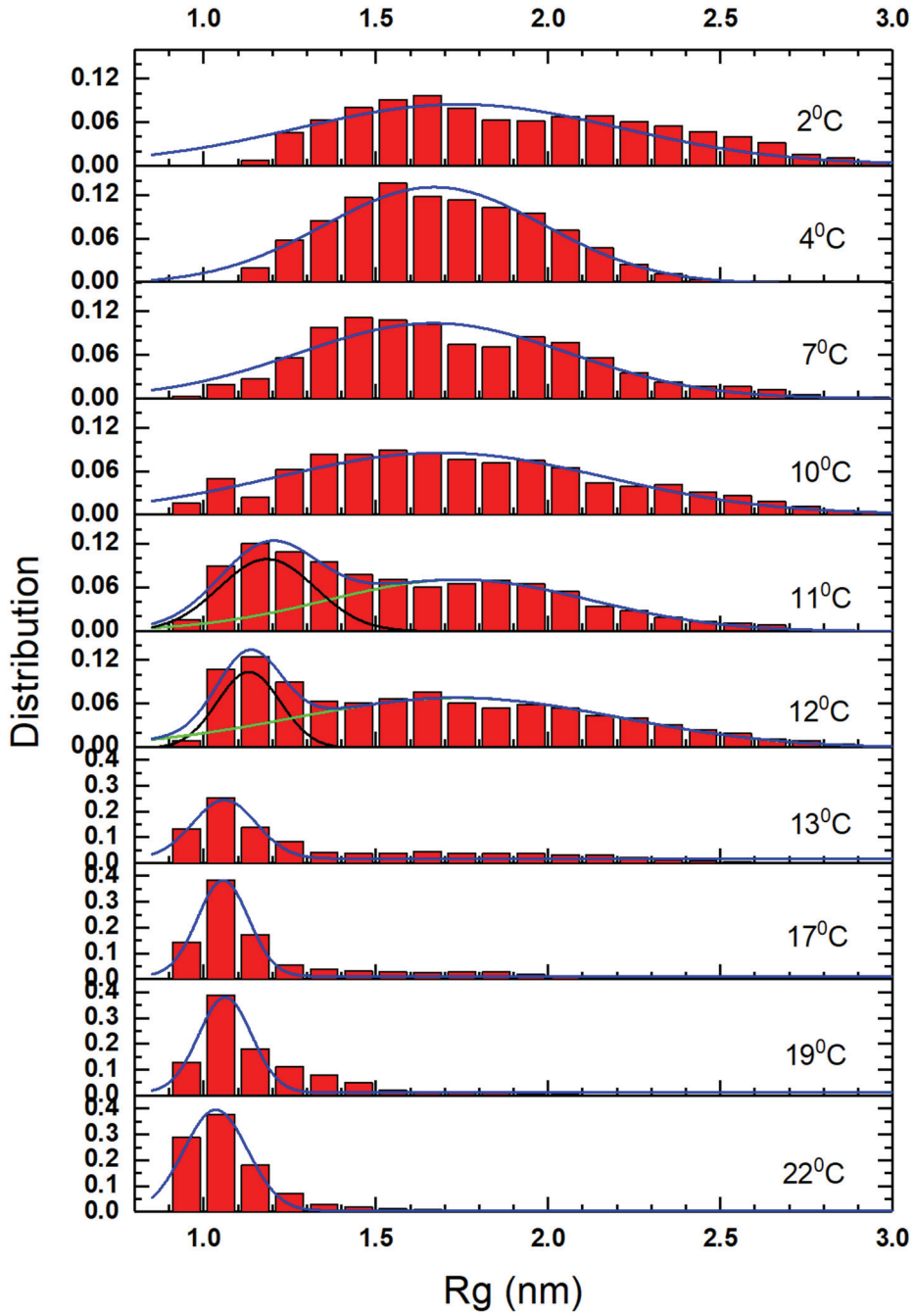


Figure 1: Statistical occurrence of the radius of gyration for PPO-4000 in aqueous solutions at different temperatures.

The average number of hydrogen bonds between water and PPO and their distribution (sequence) along the chain are important for understanding of the mechanism behind the temperature induced coil-globule transition of PPO in aqueous solutions [33]. As the temperature increases PPO loses hydrogen bonds and the distribution of non-hydrogen bonded (NHB) units along the main chain is changed. While at lower temperatures NHB units are well separated from

each other, with a temperature increase the NHB units tend to group together and form long lived hydrophobic clusters facilitating the collapse of the molecule at higher temperature [33]. Longer PPO chains produce larger NHB clusters resulting in coil-globule transformation at lower temperature.[33] While PPO exhibits a strong conformational dependence on temperature in aqueous solution, polyethylene oxide (PEO) is more hydrophilic and its conformation shows only slight changes within the same temperature range (Figure S4 of Supplementary material).

It is informative to compare the temperature dependence of PPO hydration with that for polyethylene oxide (PEO) in aqueous solutions. For comparison we used PPO-2000 (35 repeat units) and PEO36 (36 repeat units). [30] Some water molecules form single bonds ("singly bonded water") via one of the hydrogens with the oxygens of PPO or PEO while some waters formed two bonds ("doubly bonded water") with different oxygens of PPO or PEO. PEO is more hydrophilic and forms on average 1.2 hydrogen bonds per repeat unit, [30] while PPO has only about 0.8 hydrogen bonds in the hydrated state at low temperature. Among those waters hydrogen bonded to PEO on average 40% form two bonds, [30] i.e. doubly bonded, while for PPO the fraction of doubly bonded water is considerably smaller, about 7% (Figure 2). Thus, the hydration of PPO relies mainly on singly bonded water. The dynamics of singly bonded hydrating water is found to be very similar for PPO and PEO (Figure S5 of Supplementary material), as is expected in dilute solution. With a temperature increase the hydration of both polymers starts to diminish but to different extents. As shown in Figure 2a, for PPO the total number of waters hydrogen bonded to PPO systematically decreases together with singly bonded waters (Figure 2b), which represent 93% of hydrogen bonds. The percentage of doubly bonded waters remains practically unchanged. As temperature increases up to 50 °C, PPO loses nearly 17% of all hydrogen bonded water and undergoes a coil to globular transition (Figure S4). In contrast, PEO essentially does not lose any hydrogen bonded water during the same temperature change (Figure 2a) and remains well-hydrated, even though the number of hydrogen bonds decreases (Figure S4a of Supplementary material). This is achieved by the conversion of doubly bonded water to singly bonded (Figure 2c). Therefore the difference in the behavior of PPO and PEO with a temperature increase is attributed to a different mechanisms of hydration (besides differences in intrinsic hydrophobicity): for PEO doubly bonded water plays an important role and its conversion to singly bonded water allows the PEO to maintain the same number of hydrogen bonded waters, while losing some fraction of hydrogen bonds. For PPO doubly bonded water represents a rather small fraction (~7%) of all water hydrogen bonded to PPO and a decrease of hydrogen bonds with the temperature increase is achieved at expense of singly bonded water loss accompanied by conformational change from an expanded to collapsed conformation.

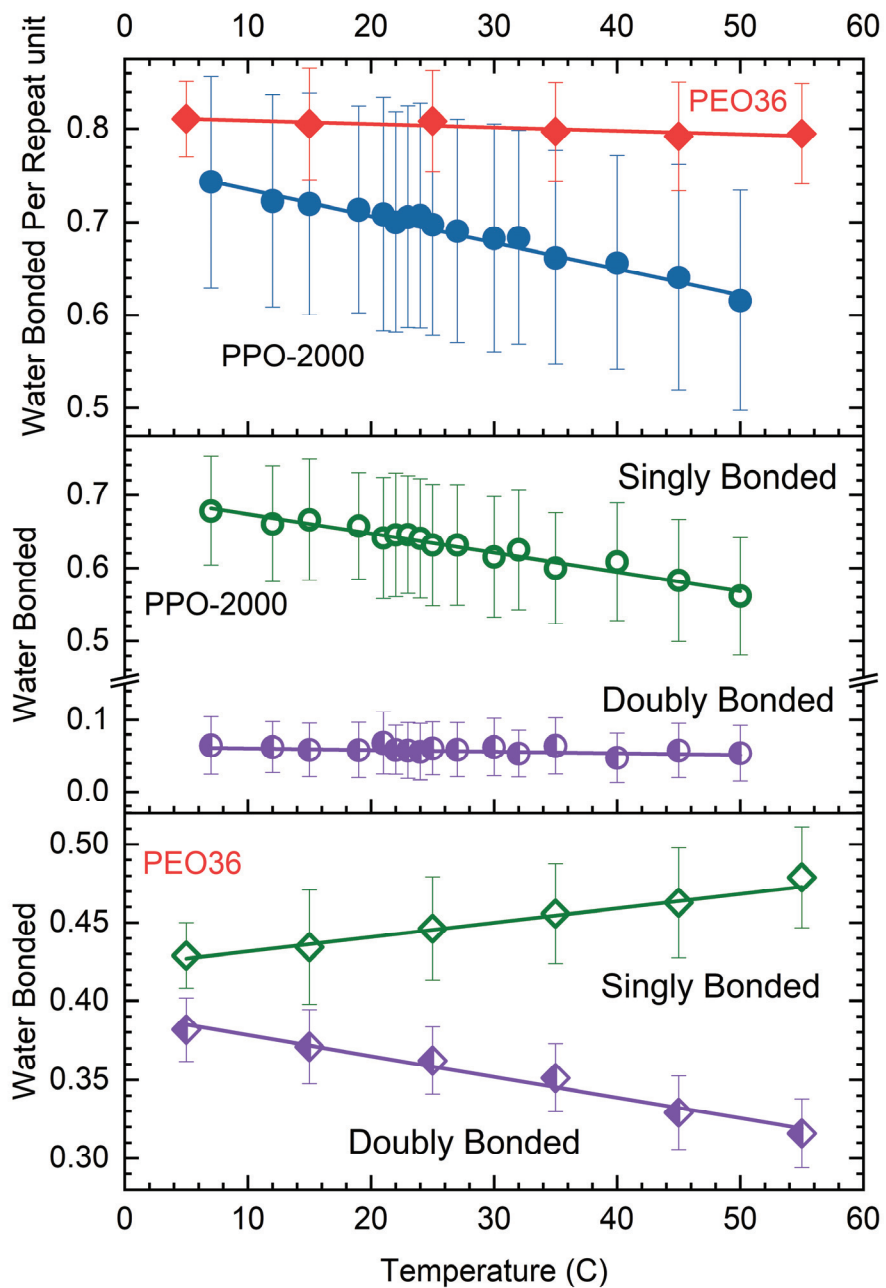


Figure 2: Temperature dependence of a) total hydrogen bonded waters per repeat unit of PPO-2000 ($N=35$) (blue circles) and PEO-1600 ($N=36$) (red diamonds); b) singly bonded (green open circles) and doubly bonded (purple half-filled circles) waters per PPO repeat unit, c) singly bonded (green open diamonds) and doubly bonded (purple half-filled diamonds) to PEO water per repeat unit.

Besides the temperature induced coil-globule transition, conformational changes in PPO can also be induced by adding a co-solvent. Here we study the effect of addition of isobutyric acid (IBA) on the PPO conformation in mixed water/IBA solvent at $T= 11^{\circ}\text{C}$. We note that at this temperature the PPO molecule is close to the coil-globule transition temperature of $T= 12^{\circ}\text{C}$ [24,33,48]. Therefore at $T= 11^{\circ}\text{C}$ PPO molecule explores both coil and globule conformation spending about 70% of the time in an expanded state and 30% in the collapsed state (Figure 1). The change in the radius of gyration of PPO as a function of the volume fraction of IBA in mixed solvent is shown in Figure 3 along with the average fraction of hydrogen bonds between solvent (water or IBA) and polymer calculated per repeat unit of PPO. As is seen, even the smallest amount of IBA added to the solvent affects the conformation of PPO. With addition of IBA, PPO-4000 collapses and reaches a minimum R_g value of 1.07 nm, corresponding to the collapsed state at a IBA volume fraction of about 0.005. Accordingly, the anisotropy strongly decreases reaching practically zero, consistent with a compact spherical globule (Figure S6 of Supplementary material). As seen in Figure 3b, the addition of IBA causes a strong reduction in the number of hydrogen bonds between PPO and water. Afterwards as the IBA volume fraction increases along with the number of hydrogen bonds between PPO and IBA, the R_g of PPO-4000 starts to increase along with the chain anisotropy (Figure S6 of Supplementary material) and stabilizes reaching the plateau of $R_g= 2.0$ nm at the volume fraction of IBA of about 0.2. The region between IBA volume fraction 0.15 and 0.9 (Figure 3 vertical dashed lines) is the two phase coexistence region [52] where the R_g of PPO is constant and similarly the hydrogen bonds between PPO-water (0.25 hydrogen bonds per repeat unit) and PPO-IBA (0.25 hydrogen bonds per repeat unit) show little change, except for a slight increase in IBA-PPO hydrogen bonding and slight decrease in water-IBA hydrogen bonding above 0.6 volume fraction of IBA. Since the PPO collapse happens around an IBA volume fraction of 0.005 in the one phase region, we conclude that the conformational transition is not related to the phase separation of the solvent. Similar to the temperature induced coil-globule transition, the co-solvent effect on conformational change of PPO is fully reversible (Figure S7).

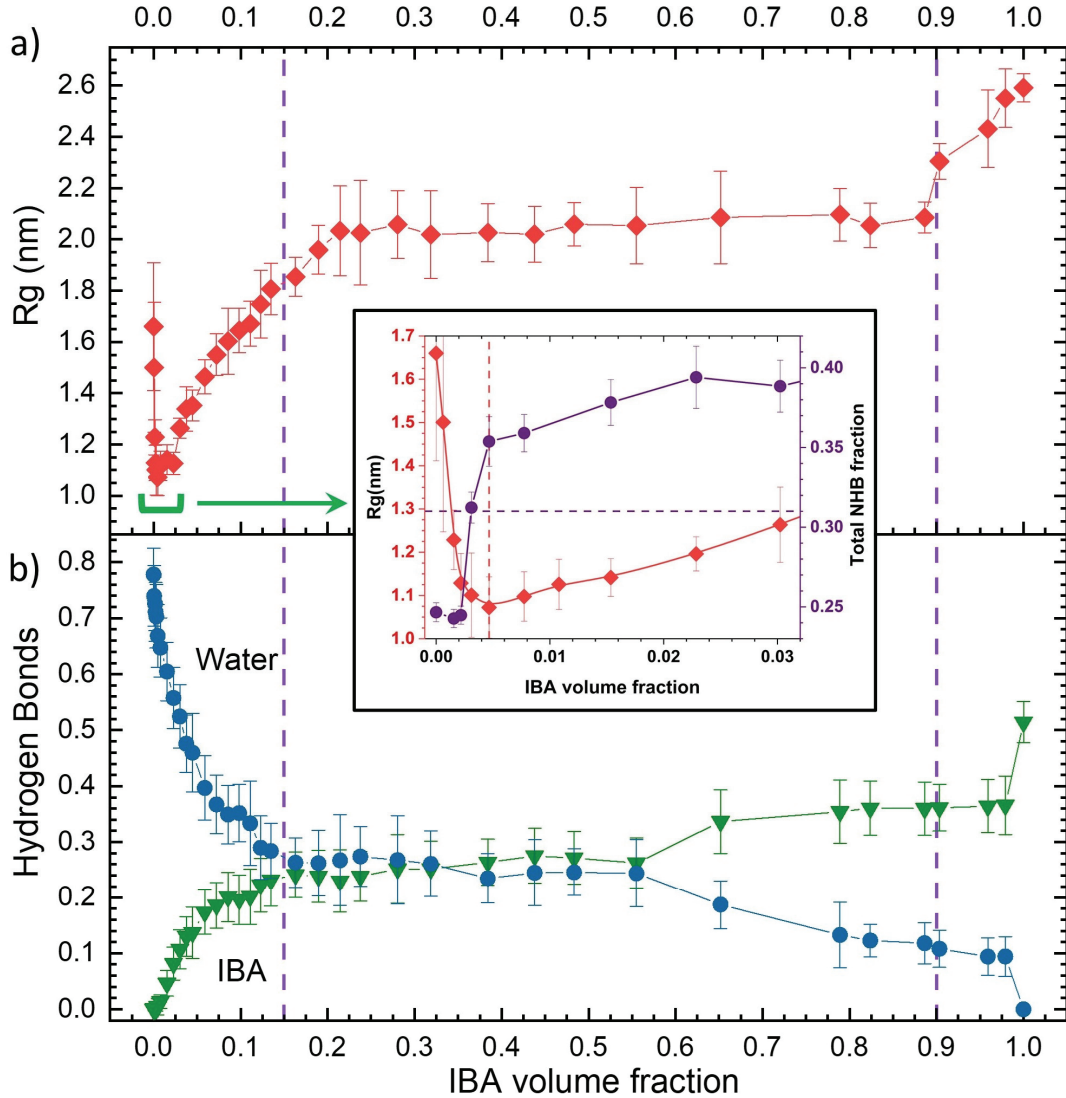


Figure 3: (a) The average radius of gyration (red diamonds) and (b) the average number of hydrogen bonds between PPO-4000 and IBA (green triangles) or water (blue circles) as functions of IBA volume fraction in solution. Vertical dashed lines enclose the two phase region of the solution. (Inset) The average radius of gyration (red diamonds) and the average fraction of non-hydrogen bonded (NHB) PPO monomers (blue circles) as functions of IBA volume fraction in the transition region.

To understand the physical origin of PPO collapse upon addition of a small amount of IBA, we analyzed trajectories with regard to the PPO conformation and hydrogen bonding between IBA and PPO at an IBA volume fraction of 0.0015 (Figure 4). We noticed a clear correlation between the presence of a hydrogen bond between PPO and IBA and the compact globule conformation of PPO, while when an IBA molecule moves away the PPO expands back to a coil conformation. From these trajectories we also notice that IBA remains hydrogen bonded to PPO for a prolonged time. We calculated the residence time correlation function $C(t)$ for IBA and water hydrogen bonded to PPO at IBA volume fraction of 0.008 (Figure S8) and fitted it with a double exponential

function. We found that 94% of IBAs hydrogen bonded to PPO have a hydrogen bond lifetime of 336ps while for waters hydrogen bonded to PPO 70% have a hydrogen bond lifetime of 44ps and 30% have a 557ps lifetime (Table S5). This indicates that on average IBA forms more stable hydrogen bonds with PPO compared to water-PPO hydrogen bonds.

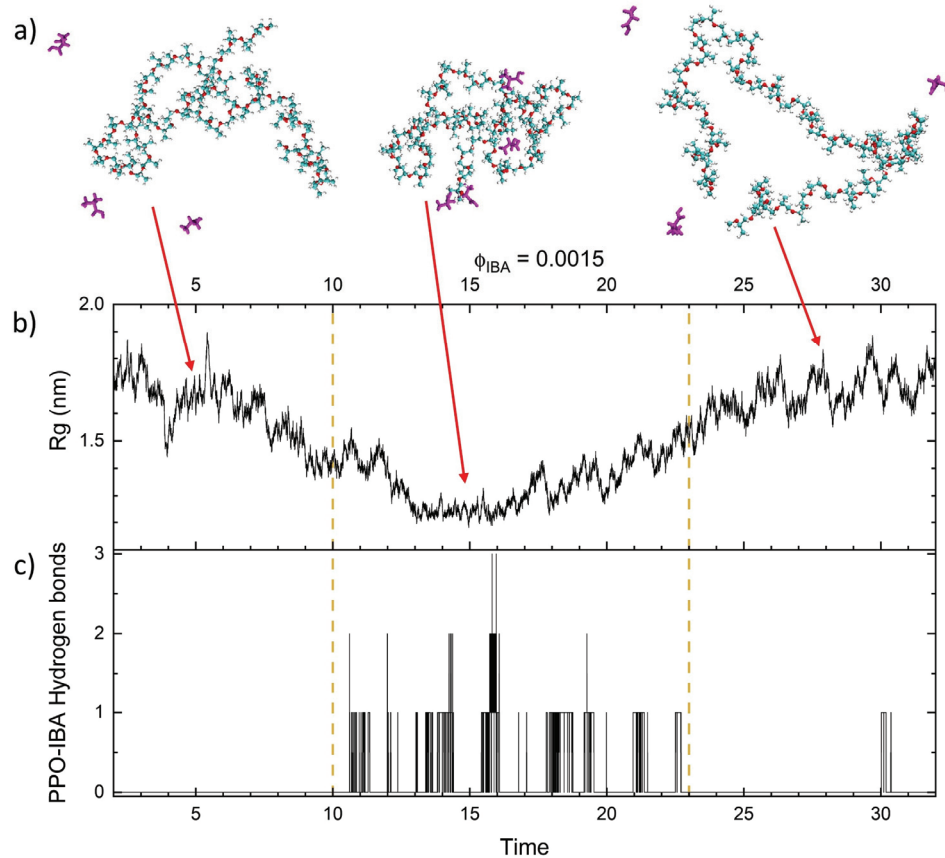


Figure 4: a) Computer simulation snapshots of PPO in water/IBA mixed solvent with an IBA volume fraction of 0.0015 at different times (arrow points to the corresponding time and R_g). b) The radius of gyration R_g of PPO 4000 and c) the number of hydrogen bonds between IBA and PPO as functions of time.

Further insights on the conformational transition of PPO upon IBA addition can be obtained by analysing the hydration shell of the polymer, which was defined as solvent molecules that are located within a 3.5 Å distance of the PPO carbons and oxygens. In pure water there are on average 1.8 water molecules in the hydration shell per PPO repeat unit, which is consistent with experimental estimates. [53] With addition of IBA the number of waters in the PPO hydration shell quickly decreases while the number of contacts that PPO makes with IBA rapidly increases (Figure 5a). This is consistent with a substantial decrease of hydrogen bonding with water upon addition of IBA as seen from Figure 3. The loss of hydrogen bonding and contacts with water implies a decrease in PPO hydration and an increase in the number of effectively hydrophobic, non-hydrogen bonded (NHB) monomers, as shown in Figure 3 inset. This decrease in hydration contributes to the observed chain collapse, but does not completely explain the mechanism of

the transition, as dehydration continues at higher IBA concentrations when the PPO conformation becomes expanded. Looking at the trajectory shown in Figure 4, we notice that having hydrogen bonding with IBA is another factor contributing to the conformational transition. Indeed the IBA molecule itself is amphiphilic similar to PPO and its solubility in water relies of hydrogen bonding as well. Thus, the affinity of IBA to PPO comes as no surprise. Indeed, analyzing the fraction of IBA in the hydration shell of PPO as shown in Figure 5b one can see that it is much higher than the average fraction of IBA in solution. As IBA hydrogen bonded to PPO can be viewed as essentially hydrophobic and longlived (Figures S5 and S8), it acts as nucleation site for PPO collapse (Figure 4), which in turn attracts more IBA molecules (due to favorable volume interactions) in the vicinity of PPO. When the fraction of IBA in the hydration shell exceeds 0.3 and there is on average more than 1 IBA molecule hydrogen bonded to PPO (Figure 5) the polymer collapses into a globule. It is interesting to note that the fraction of non-hydrogen bonded (NHB) units exceeds 0.3 at that point similar to what occurs at the the coil-globule transition temperature for PPO,[33] even though the mechanism of PPO collapse upon addition of IBA is different than that induced by a temperature increase. In the latter case an increase in the length of a sequence of non-hydrogen bonded units with an increase in temperature makes PPO behave as effectively a block-copolymer, stimulating the transition. [33] While here the stable hydrogen bonding with the essentially hydrophobic IBA molecules nucleates the conformational transition of partially dehydrated polymer.

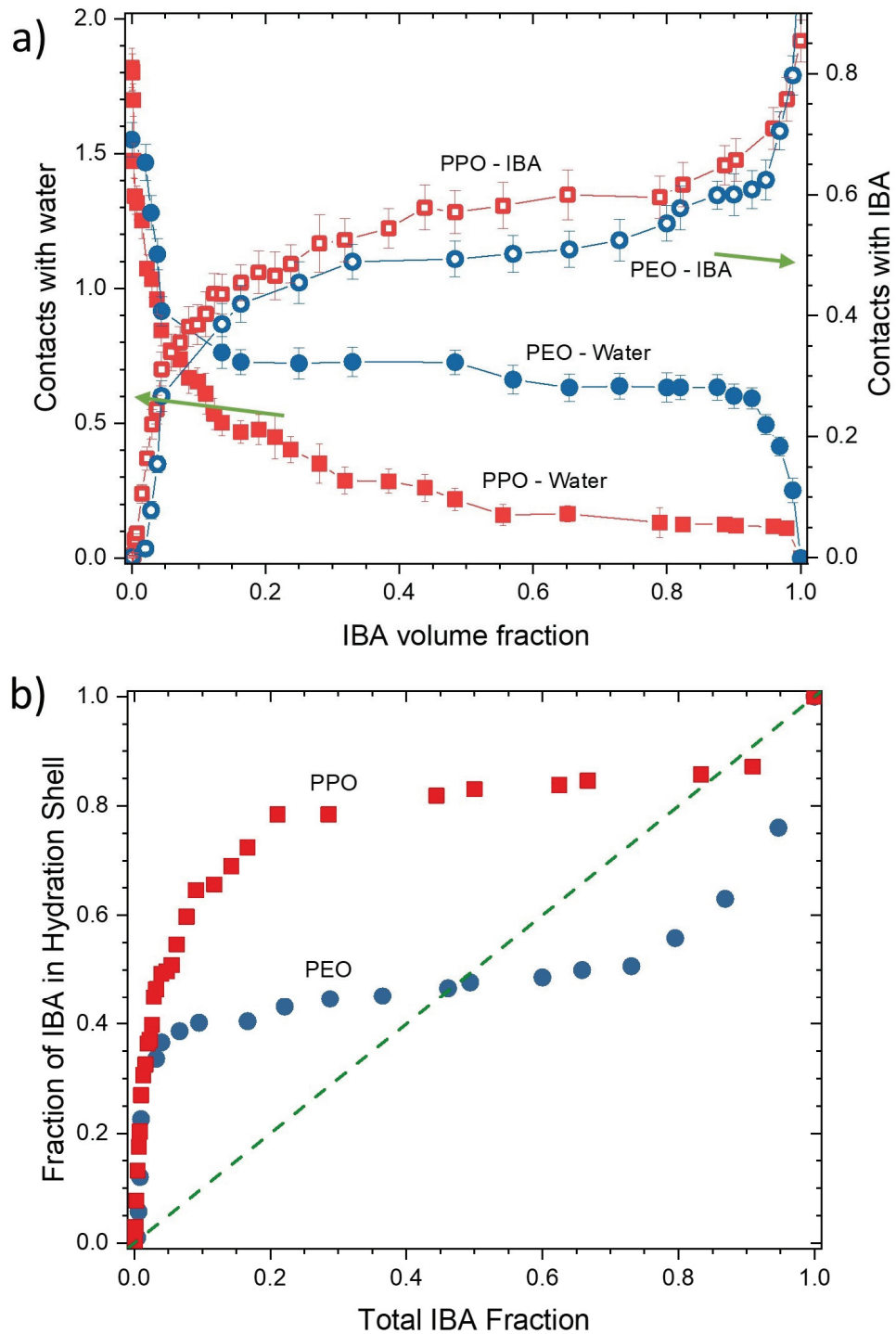


Figure 5: a) Average number of water molecules (solid symbols) and IBA molecules (open symbols) in the polymer hydration shell per repeat unit of PPO (red squares) or PEO (blue circles) as functions of the IBA volume fraction. b) The fraction of IBA in the hydration shell of PPO (red squares) and PEO (blue circles) as functions of the overall average fraction of IBA in solution.

Looking at the statistical occurrence of the PPO conformations as shown in Figure 6 for different IBA volume fractions in solution it is further evident that IBA has a significant impact on the conformation of PPO. The conformational behavior of PPO at a very low IBA concentration is similar to that in pure water at 11C, where it is bimodal (Figure 1). The presence of even a very small amount of IBA shifts the bimodal peaks to slightly lower values: 1.1nm and 1.6nm. As the IBA volume fraction increases the PPO size distribution changes from a bimodal to a homogeneous narrowly distributed one corresponding to a collapsed state. In the collapsed state PPO is hydrogen bonded to at least one IBA molecule, which further attracts more IBA molecules to the PPO vicinity. As the IBA concentration increases more hydrogen bonds form between IBA and PPO and the number of IBA molecules in the hydration shell of PPO further increases creating a locally more hydrophobic IBA-rich zone. By wrapping itself around the local IBA-rich pool, PPO can benefit from its affinity to IBA in its hydration shell while at the same time maintaining some hydrogen bonding with water (Figure 7). With an increase in the number of IBA molecules in the pool near the PPO, the polymer forms more hydrogen bonds with IBA and starts to expand experiencing a different local environment. The R_g of PPO (Figures 3, 6 and 7) and fraction of IBA in hydration shell of PPO (Figure 5) keep increasing until the IBA volume fraction reaches about 0.15 at which point the IBA starts to phase separate from water and the level of hydrogen bonding with water and IBA becomes comparable: about 0.25 each per repeat unit of PPO (Figure 3). The fraction of IBA in the hydration shell continues to increase until it plateaus at 0.8 when the average volume fraction of IBA is about 0.2. Accordingly, PPO resides at the interface between the IBA-rich region and water-rich regions of the phase separated state in a slightly expanded conformation compared to that in pure aqueous solution (Figure 7). When the volume fraction of IBA reaches about 0.6, PPO starts to further lose hydrogen bonding with water (Figures 3 and 7). Above a volume fraction 0.9 of IBA the solution once again becomes homogeneous and the PPO conformation becomes even more expanded with asphericity reaching 1 (Figure S6 of Supplementary material) indicating highly asymmetric conformation when PPO is solvated by IBA alone (Figures 3 and 7).

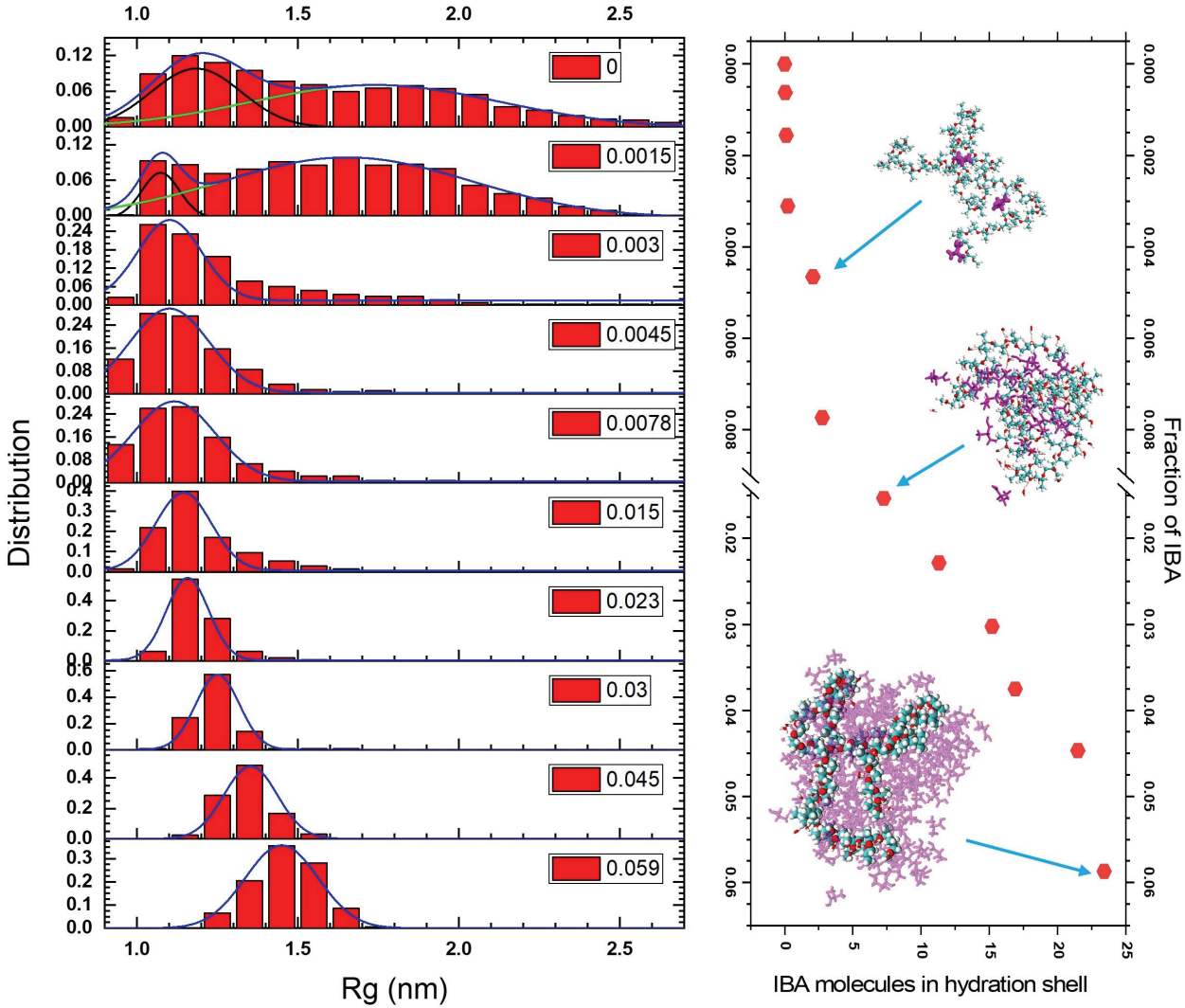


Figure 6: (left) Statistical occurrence of the radius of gyration of PPO-4000 in IBA/water solution at the indicated IBA volume fraction and (right) the number of IBA in the hydration shell of PPO-4000 in mixed solvent at different IBA volume fractions along with MD simulation snapshots of PPO conformation and IBA molecules (shown in magenta) in the PPO vicinity.

As discussed above, PEO is more water soluble and forms a larger number of hydrogen bonds with singly and doubly bonded water compared to PPO (Figure 2). It is informative to compare the conformational changes of these polymers in mixed IBA/water solvent. For both polymers addition of a small amount of IBA to aqueous solution results in a significant loss of hydrogen bonds and dehydration (Figures 5a and 7b). Indeed adding 0.1 volume fraction of IBA reduces the average number of water molecules in the hydration shell by half or more (Figure 5a) for both polymers, while hydrogen bonds decrease by 25% for PEO and 60% for PPO. Accordingly, the radius of gyration of PEO slightly decreases, while the PPO chain collapses (Figure 7a), as discussed above. Obviously, the stronger and more stable hydrogen bonds contributed by doubly-bonded water leads to higher PEO hydration in water and higher retention of water in

the presence of IBA leading to the minor conformational change observed. In contrast, PPO for which its solubility is based primarily on weaker singly bonded water, already explores both the expanded and collapsed conformations at 11C even before IBA addition, which leads to further dehydration of the polymer and shifts equilibrium towards the collapsed state. It is interesting to note that for both polymers the IBA presence in the hydration shell far exceeds the average fraction of IBA in solution, confirming the affinity of IBA for both polymers (Figure 5b).

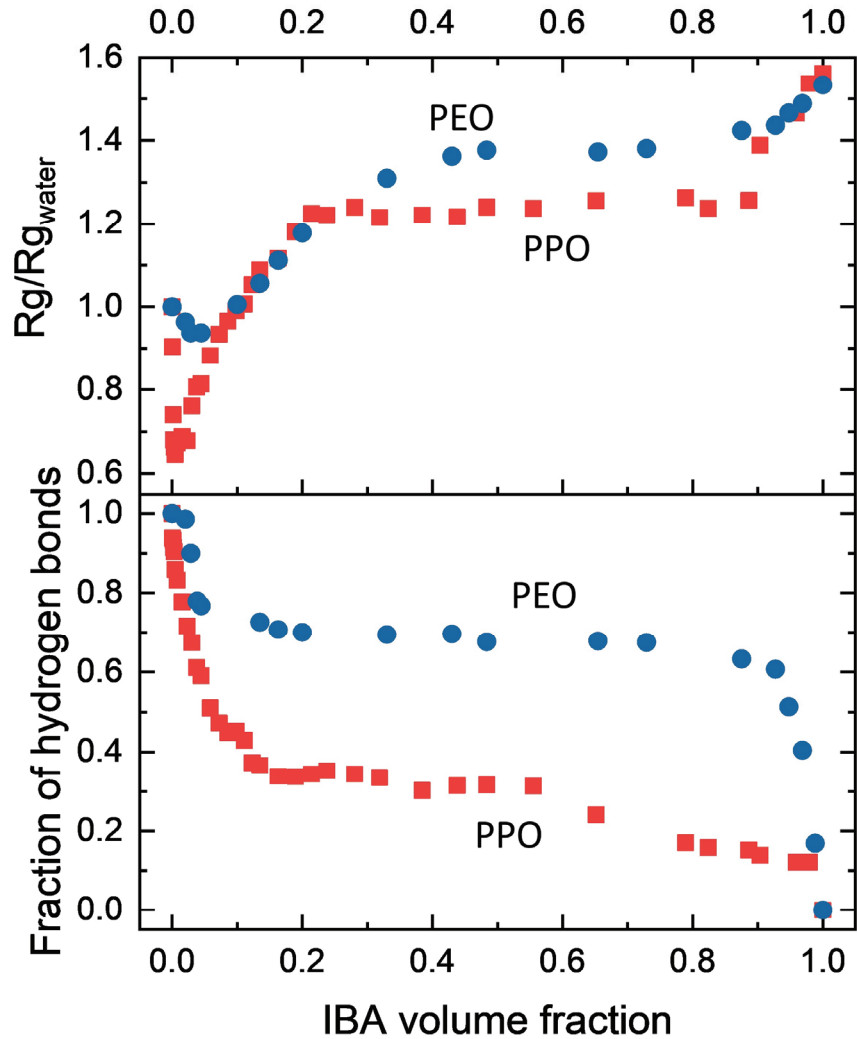


Figure 7: a) The ratio of Rg of the polymer in mixed solvent to that in pure water Rg_{water} and b) the ratio of the average number of hydrogen bonds between water and polymer in mixed solvent to that in pure water for PPO (red squares) and PEO (blue circles) as functions of the average fraction of IBA in solution.

With a further increase of IBA in solution the polymer conformations start to expand and reach a plateau in the two phase region of IBA-water when the fraction of IBA in the hydration shell of PEO stabilizes at 0.4 and for PPO at 0.8 (Figure 7a and 5b). In this region PEO is 1.4 times more expanded than in aqueous solutions, retains 80% of hydrogen bonds with water (Figure 7b) and is located within the IBA phase but with some water remaining in the hydration shell around the polymer (Figure 8b). In contrast PPO localized at the interface between IBA and water (Figure 8a), is 1.2 times more expanded than in aqueous solution while retaining only 30% of hydrogen bonds with water and continues losing hydrogen bonds with water when the IBA volume fraction exceeds 0.6. When the volume fraction of IBA exceeds 0.9 in the IBA-dominated one phase region both polymers lose hydrogen bonds with water and further expand (Figure 7). In pure IBA solution PEO forms a helical structure [29,30] with nearly one hydrogen bond with IBA per repeat unit, i.e. nearly all oxygens of PEO are hydrogen bonded to IBA in a “bottle-brush like” arrangement (Figure 8d). PPO also forms an expanded conformation in pure IBA, except on average only each other oxygen is hydrogen bonded to IBA, possibly due to obstruction by methyl groups (Figure 8c).

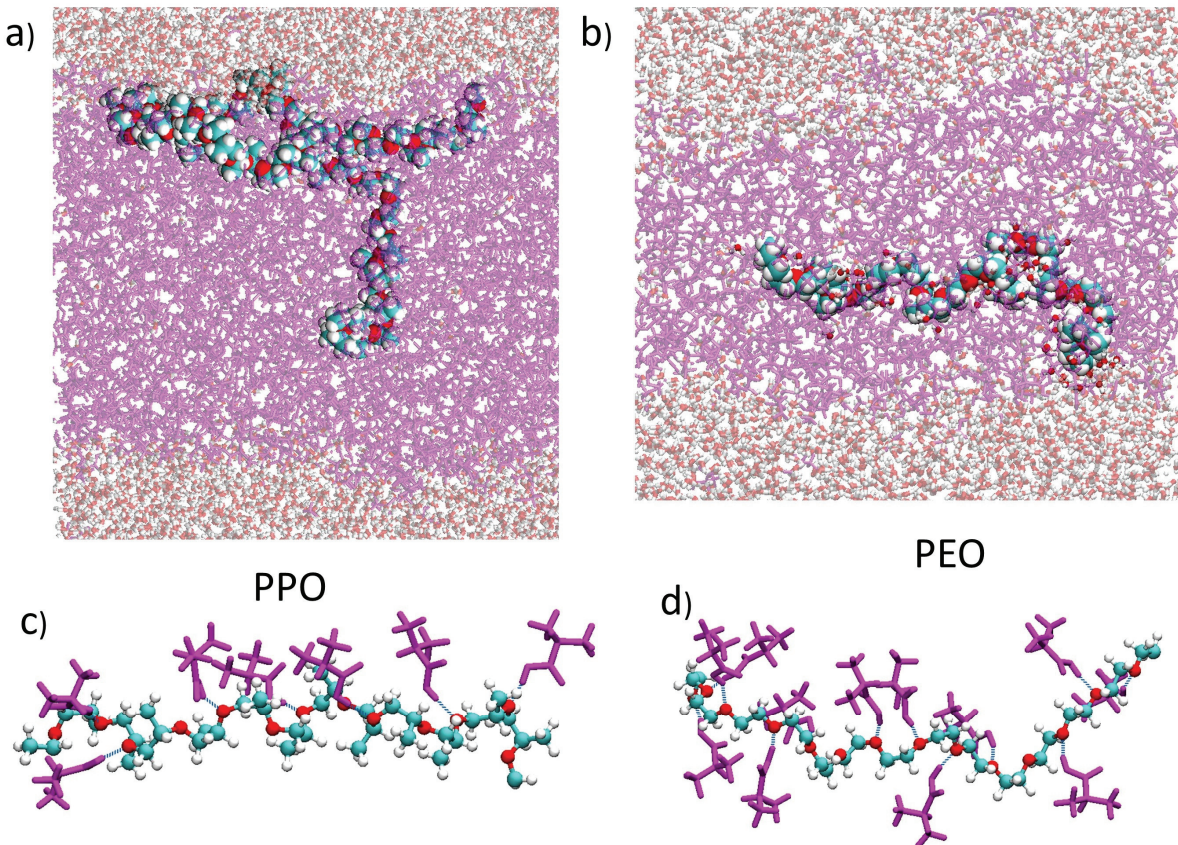


Figure 8: Computer simulation snapshots of: a) PPO located at the interface between IBA-rich and water-rich phases and b) PEO located within the IBA-rich phase together with hydrating water in mixed IBA/water solvent with volume fraction of IBA 0.5. Computer simulation snapshot of a

section of c) PPO and d) PEO chains together with IBA molecules hydrogen bonded to polymers in pure IBA solution. Carbon atoms are shown in cyan, oxygens in red, hydrogens in white, IBA molecules are shown in magenta and the hydrogen bonds in dashed blue lines.

4. Conclusions

The atomistic molecular dynamics simulations discussed in this paper provide insights into the delicate balance of hydrogen bonding and volume interactions by investigating PPO and PEO conformational changes in response to temperature variation or co-solvent addition. Closer to the coil-globule transition region of PPO we observed that PPO explores both the coil and globule states spending 30% of the time in the globule and 70% in the coil state, as seen in the polymer size distribution (Figure 1 and 6). The comparison with PEO shows that such strong sensitivity of PPO to temperature or co-solvent is a result of not only the higher hydrophobicity of PPO, but also the difference in hydrogen bonding. PPO forms a smaller number of hydrogen bonds with water than PEO and furthermore these bonds are less stable, as the vast majority are due to singly bonded water. In contrast, about 40% of the hydrogen bonds between PEO and water is formed by the more stable doubly bonded water. As a result, for PEO when the temperature increases the doubly bonded water converts into a singly bonded water by losing one of the two hydrogen bonds such that PEO remains hydrogen bonded to the same number of water molecules, which contribute to its hydration (Figure 2). Therefore, as the temperature increases PEO remains fully hydrated and soluble in water showing little effect on its conformation until it reaches very high temperature. In contrast, PPO which is mainly hydrated by singly bonded water, starts to lose its hydrogen bonds together with hydrating water upon a temperature increase and undergoes a coil-globule transition when about 30% of its monomers become dehydrated.

Upon addition of a rather small amount of isobutyric acid (IBA) to aqueous solution we observed an abrupt collapse of PPO followed up by a slow recovery of its coil conformation and further expansion as the IBA fraction increases (Figure 3). We investigated the molecular details of the conformational changes of PPO and found that stable hydrogen bonds with IBA and loss of hydrogen bonds with water are the main contributing factors to the IBA-induced collapse. Being an amphiphilic molecule, like PPO, IBA has tendency to accumulate in the vicinity of PPO (Figure 5) consequently decreasing the hydrogen bonding between PPO and water. A stable IBA-PPO hydrogen bond creates a nucleation site stimulating PPO to gather around hydrophobic monomers which are not hydrogen bonded (NHB) with water (Figure 4). Once the total fraction of NHBs monomers exceeds 0.3 the polymer collapses (Figure 6) similar to the temperature-induced coil-globular transition [33]. With further IBA addition, as more IBA molecules aggregate around PPO, the polymer locates at the interface between IBA and water in order to form hydrogen bonds with both IBA and water and starts to expand (Figures 6 and 7). Somewhat similar behavior is observed for PEO upon IBA addition, except PEO does not collapse and locates in the IBA-rich region while maintaining its hydration shell. Indeed, comparing PEO and PPO within the two phase region (Figure 7), one can notice that PEO retains 80% of its hydrogen bonds with water compared to aqueous solution even when being within the IBA-rich region, while PPO has fewer than 40% of hydrogen bonds with water while located at the interface between IBA

and water. The difference in the behavior of these two related polymers (besides their intrinsically different hydrophobicity) is likely a result of the doubly bonded water that travels together with PEO into the IBA-rich region, while PPO has only the less stable singly bonded water. At high IBA concentration both polymers become dehydrated and expand, with PEO forming on average 0.8 hydrogen bonds with IBA per repeat unit in a helical conformation and PPO forming 0.5 hydrogen bonds with IBA in an expanded state (Figure 8). The comparative response of PPO and PEO to the addition of co-solvent illustrates that differences in hydrogen bonding and a polymer's capability to maintain its hydration shell are the key factors in polymer responsiveness to external triggers such as solvent or temperature change, which should be taken into consideration upon responsive material design and applications.

Corresponding Author:

Elena E. Dormidontova – Polymer Program, Institute of Materials Science and Physics Department, University of Connecticut, Storrs, Connecticut 06269, United States. Orcid: 0000-0002-7669-8957. Email: elena@uconn.edu

Acknowledgements

This research is supported by the National Science Foundation under Grant No. DMR-1916864.

Supplementary material

Supplementary data containing additional simulation details and data analysis for this article can be found online at ...

References

- [1] Y.J. Kim, Y.T. Matsunaga, Thermo-responsive polymers and their application as smart biomaterials, *J. Mater. Chem. B*. 5 (2017) 4307–4321. <https://doi.org/10.1039/c7tb00157f>.
- [2] M. Karimi, P. Sahandi Zangabad, A. Ghasemi, M. Amiri, M. Bahrami, H. Malekzad, H. Ghahramanzadeh Asl, Z. Mahdieh, M. Bozorgomid, A. Ghasemi, M.R. Rahmani Taji Boyuk, M.R. Hamblin, Temperature-Responsive Smart Nanocarriers for Delivery of Therapeutic Agents: Applications and Recent Advances, *ACS Appl. Mater. Interfaces*. 8 (2016) 21107–21133. <https://doi.org/10.1021/acsami.6b00371>.
- [3] M.A. Ward, T.K. Georgiou, Thermoresponsive polymers for biomedical applications, *Polymers (Basel)*. 3 (2011) 1215–1242. <https://doi.org/10.3390/polym3031215>.
- [4] A. Pitt-Barry, N.P.E. Barry, Pluronic® block-copolymers in medicine: From chemical and biological versatility to rationalisation and clinical advances, *Polym. Chem.* 5 (2014) 3291–3297. <https://doi.org/10.1039/c4py00039k>.
- [5] H.-J. Huang, Y.-L. Tsai, S.-H. Lin, S. Hsu, Smart polymers for cell therapy and precision medicine, *J. Biomed. Sci.* 26 (2019) 73. <https://doi.org/10.1186/s12929-019-0571-4>.

[6] G. Zhang, C. Wu, The water/methanol complexation induced reentrant coil-to-globule-to-coil transition of individual homopolymer chains in extremely dilute solution, *J. Am. Chem. Soc.* 123 (2001) 1376–1380. <https://doi.org/10.1021/ja003889s>.

[7] F. Tanaka, T. Koga, F.M. Winnik, Temperature-responsive polymers in mixed solvents: Competitive hydrogen bonds cause cononsolvency, *Phys. Rev. Lett.* 101 (2008). <https://doi.org/10.1103/PhysRevLett.101.028302>.

[8] M.J.A. Hore, B. Hammouda, Y. Li, H. Cheng, Co-nonsolvency of poly(n-isopropylacrylamide) in deuterated water/ethanol mixtures, *Macromolecules.* 46 (2013) 7894–7901. <https://doi.org/10.1021/ma401665h>.

[9] D. Mukherji, C.M. Marques, K. Kremer, Polymer collapse in miscible good solvents is a generic phenomenon driven by preferential adsorption, *Nat. Commun.* 5 (2014) 1–6. <https://doi.org/10.1038/ncomms5882>.

[10] D. Mukherji, C.M. Marques, T. Stuehn, K. Kremer, Co-non-solvency: Mean-field polymer theory does not describe polymer collapse transition in a mixture of two competing good solvents, *J. Chem. Phys.* 142 (2015). <https://doi.org/10.1063/1.4914870>.

[11] D. Mukherji, M. Wagner, M.D. Watson, S. Winzen, T.E. De Oliveira, C.M. Marques, K. Kremer, Relating side chain organization of PNIPAm with its conformation in aqueous methanol, *Soft Matter.* 12 (2016) 7995–8003. <https://doi.org/10.1039/c6sm01789d>.

[12] D. Mukherji, K. Kremer, How does poly(N-isopropylacrylamide) trigger phase separation in aqueous alcohol?, *Polym. Sci. - Ser. C.* 59 (2017) 119–124. <https://doi.org/10.1134/S181123821701009X>.

[13] H.A. Pérez-Ramírez, C. Haro-Pérez, E. Vázquez-Contreras, J. Klapp, G. Bautista-Carbalal, G. Odriozola, P-NIPAM in water-acetone mixtures: Experiments and simulations, *Phys. Chem. Chem. Phys.* 21 (2019) 5106–5116. <https://doi.org/10.1039/c8cp07549b>.

[14] H.A. Pérez-Ramírez, C. Haro-Pérez, G. Odriozola, Effect of Temperature on the Cononsolvency of Poly(N-isopropylacrylamide) (PNIPAM) in Aqueous 1-Propanol, *ACS Appl. Polym. Mater.* 1 (2019) 2961–2972. <https://doi.org/10.1021/acsapm.9b00665>.

[15] Y.A. Budkov, A.L. Kolesnikov, N.N. Kalikin, M.G. Kiselev, A statistical theory of coil-to-globule-to-coil transition of a polymer chain in a mixture of good solvents, *Epl.* 114 (2016) 0–6. <https://doi.org/10.1209/0295-5075/114/46004>.

[16] Y.A. Budkov, A.L. Kolesnikov, Models of the Conformational Behavior of Polymers in Mixed Solvents, *Polym. Sci. - Ser. C.* 60 (2018) 148–159. <https://doi.org/10.1134/S1811238218020030>.

[17] S. Bharadwaj, N.F.A. Van Der Vegt, Does Preferential Adsorption Drive Cononsolvency?, *Macromolecules.* 52 (2019) 4131–4138. <https://doi.org/10.1021/acs.macromol.9b00575>.

[18] S. Bharadwaj, D. Nayar, C. Dalgicdir, N.F.A. Van Der Vegt, An interplay of excluded-volume and polymer-(co)solvent attractive interactions regulates polymer collapse in mixed solvents, *J. Chem. Phys.* 154 (2021). <https://doi.org/10.1063/5.0046746>.

[19] F. Rodríguez-Ropero, T. Hajari, N.F.A. Van Der Vegt, Mechanism of Polymer Collapse in Miscible Good Solvents, *J. Phys. Chem. B.* 119 (2015) 15780–15788. <https://doi.org/10.1021/acs.jpcb.5b10684>.

[20] T. Zuo, C. Ma, G. Jiao, Z. Han, S. Xiao, H. Liang, L. Hong, D. Bowron, A. Soper, C.C. Han, H. Cheng, Water/Cosolvent Attraction Induced Phase Separation: A Molecular Picture of Cononsolvency, *Macromolecules.* 52 (2019) 457–464.

https://doi.org/10.1021/acs.macromol.8b02196.

[21] H.G. Schild, M. Muthukumar, D.A. Tirrell, Cononsolvency in Mixed Aqueous Solutions of Poly(N- isopropylacrylamide), *Macromolecules*. 24 (1991) 948–952.
https://doi.org/10.1021/ma00004a022.

[22] J. Dudowicz, K.F. Freed, J.F. Douglas, Communication: Cosolvency and cononsolvency explained in terms of a Flory-Huggins type theory, *J. Chem. Phys.* 143 (2015).
https://doi.org/10.1063/1.4932061.

[23] J. Walter, J. Sehrt, J. Vrabec, H. Hasse, Molecular dynamics and experimental study of conformation change of poly(N -isopropylacrylamide) hydrogels in mixtures of water and methanol, *J. Phys. Chem. B*. 116 (2012) 5251–5259. https://doi.org/10.1021/jp212357n.

[24] J. Armstrong, B. Chowdhry, R. O'Brien, A. Beezer, J. Mitchell, S. Leharne, Scanning microcalorimetric investigations of phase transitions in dilute aqueous solutions of poly(oxypropylene), *J. Phys. Chem.* 99 (1995) 4590–4598.
https://doi.org/10.1021/j100013a033.

[25] F. Tanaka, T. Koga, H. Kojima, F.M. Winnik, Temperature- and tension-induced coil globule transition of poly(N-isopropylacrylamide) chains in water and mixed solvent of water/methanol, *Macromolecules*. 42 (2009) 1321–1330.
https://doi.org/10.1021/ma801982e.

[26] S. Hezaveh, S. Samanta, G. Milano, D. Roccatano, Molecular dynamics simulation study of solvent effects on conformation and dynamics of polyethylene oxide and polypropylene oxide chains in water and in common organic solvents, *J. Chem. Phys.* 136 (2012).
https://doi.org/10.1063/1.3694736.

[27] M. Guettari, A. Belaïdi, S. Abel, T. Tajouri, Polyvinylpyrrolidone Behavior in Water/Ethanol Mixed Solvents: Comparison of Modeling Predictions with Experimental Results, *J. Solution Chem.* 46 (2017) 1404–1417. https://doi.org/10.1007/s10953-017-0649-0.

[28] M. Ohkura, T. Kanaya, K. Kaji, Gels of poly (vinyl alcohol) from dimethyl sulphoxide / water solutions, (n.d.).

[29] M.L. Alessi, A.I. Norman, S.E. Knowlton, D.L. Ho, S.C. Greer, Helical and coil conformations of poly(ethylene glycol) in isobutyric acid and water, *Macromolecules*. 38 (2005) 9333–9340. https://doi.org/10.1021/ma051339e.

[30] U.R. Dahal, E.E. Dormidontova, The dynamics of solvation dictates the conformation of polyethylene oxide in aqueous, isobutyric acid and binary solutions, *Phys. Chem. Chem. Phys.* 19 (2017) 9823–9832. https://doi.org/10.1039/c7cp00526a.

[31] E.E. Dormidontova, Influence of end groups on phase behavior and properties of PEO in aqueous solutions, *Macromolecules*. 37 (2004) 7747–7761.
https://doi.org/10.1021/ma035609.

[32] E.E. Dormidontova, Role of competitive PEO-water and water-water hydrogen bonding in aqueous solution PEO behavior, *Macromolecules*. 35 (2002) 987–1001.
https://doi.org/10.1021/ma010804e.

[33] R. Dahanayake, E.E. Dormidontova, Hydrogen Bonding Sequence Directed Coil-Globule Transition in Water Soluble Thermoresponsive Polymers, *Phys. Rev. Lett.* 127 (2021) 167801. https://doi.org/10.1103/physrevlett.127.167801.

[34] Y. Mao, Y. Zhang, Thermal conductivity, shear viscosity and specific heat of rigid water

models, *Chem. Phys. Lett.* 542 (2012) 37–41.
<https://doi.org/10.1016/j.cplett.2012.05.044>.

[35] P. Mark, L. Nilsson, Structure and dynamics of the TIP3P, SPC, and SPC/E water models at 298 K, *J. Phys. Chem. A.* 105 (2001) 9954–9960. <https://doi.org/10.1021/jp003020w>.

[36] W.L. Jorgensen, D.S. Maxwell, J. Tirado-Rives, Development and testing of the OPLS all-atom force field on conformational energetics and properties of organic liquids, *J. Am. Chem. Soc.* 118 (1996) 11225–11236. <https://doi.org/10.1021/ja9621760>.

[37] V.S. Neverov, A. V. Komolkin, A study of the structural and thermodynamic properties of water by the molecular dynamics method, *Russ. J. Phys. Chem. B.* 4 (2010) 217–226.
<https://doi.org/10.1134/S1990793110020065>.

[38] J.R. Schmidt, S.T. Roberts, J.J. Loparo, A. Tokmakoff, M.D. Fayer, J.L. Skinner, Are water simulation models consistent with steady-state and ultrafast vibrational spectroscopy experiments?, *Chem. Phys.* 341 (2007) 143–157.
<https://doi.org/10.1016/j.chemphys.2007.06.043>.

[39] S.P. Kadaoluwa Pathirannahalage, N. Meftahi, A. Elbourne, A.C.G. Weiss, C.F. McConville, A. Padua, D.A. Winkler, M. Costa Gomes, T.L. Greaves, T.C. Le, Q.A. Besford, A.J. Christofferson, Systematic Comparison of the Structural and Dynamic Properties of Commonly Used Water Models for Molecular Dynamics Simulations, *J. Chem. Inf. Model.* 61 (2021) 4521–4536. <https://doi.org/10.1021/acs.jcim.1c00794>.

[40] U.R. Dahal, E.E. Dormidontova, Spontaneous Insertion, Helix Formation, and Hydration of Polyethylene Oxide in Carbon Nanotubes, *Phys. Rev. Lett.* 117 (2016) 027801.
<https://doi.org/10.1103/PhysRevLett.117.027801>.

[41] U.R. Dahal, A. Prhashanna, E.E. Dormidontova, Hydration of diblock copolymer micelles: Effects of hydrophobicity and co-solvent, *J. Chem. Phys.* 150 (2019) 184908.
<https://doi.org/10.1063/1.5089251>.

[42] D. Bedrov, G.D. Smith, Molecular Dynamics Simulations of 1,2-Dimethoxypropane and 1,2-Dimethoxyethane in Aqueous Solution, *J. Phys. Chem. B.* 103 (1999) 10001–10006.
<https://doi.org/10.1021/jp991454p>.

[43] D. Bedrov, M. Pekny, G.D. Smith, Quantum-chemistry-based force field for 1,2-dimethoxyethane and poly(ethylene oxide) in aqueous solution, *J. Phys. Chem. B.* 102 (1998) 996–1001. <https://doi.org/10.1021/jp972545u>.

[44] G.D. Smith, O. Borodin, D. Bedrov, Quantum chemistry based force field for simulations of poly(propylene oxide) and its oligomers, *J. Phys. Chem. A.* 102 (1998) 10318–10323.
<https://doi.org/10.1021/jp981599g>.

[45] S. Hezaveh, S. Samanta, G. Milano, D. Roccatano, Structure and dynamics of 1,2-dimethoxyethane and 1,2-dimethoxypropane in aqueous and non-aqueous solutions: A molecular dynamics study, *J. Chem. Phys.* 135 (2011).
<https://doi.org/10.1063/1.3643417>.

[46] N. Ileri Ercan, P. Stroeve, J.W. Tringe, R. Faller, Understanding the Interaction of Pluronics L61 and L64 with a DOPC Lipid Bilayer: An Atomistic Molecular Dynamics Study, *Langmuir.* 32 (2016) 10026–10033. <https://doi.org/10.1021/acs.langmuir.6b02360>.

[47] H.G. Schild, D.A. Tirrell, Microcalorimetric detection of lower critical solution temperatures in aqueous polymer solutions, *J. Phys. Chem.* 94 (1990) 4352–4356.
<https://doi.org/10.1021/j100373a088>.

- [48] J. Armstrong, B. Chowdhry, R. O'Brien, A. Beezer, J. Mitchell, S. Leharne, On the molecular origin of the cooperative coil-to-globule transition of poly(: N-isopropylacrylamide) in water, *J. Phys. Chem. B.* 102 (1998) 1–6.
<https://doi.org/10.1039/c8cp00537k>.
- [49] A. Luzar, D. Chandler, Effect of Environment on Hydrogen Bond Dynamics in Liquid Water, *Phys. Rev. Lett.* 76 (1996) 928–931. <https://doi.org/10.1103/PhysRevLett.76.928>.
- [50] A. Luzar, D. Chandler, Hydrogen-bond kinetics in liquid water, *Nature.* 379 (1996) 55–57.
<https://doi.org/10.1038/379055a0>.
- [51] W. Humphrey, A. Dalke, K. Schulten, VMD: Visual Molecular Dynamics, *J. Mol. Graph.* 14 (1996) 33–38. <https://www.tpbiosystems.com/tap/products/index.htm>.
- [52] J. Colombani, J. Bert, Early sedimentation and crossover kinetics in an off-critical phase-separating liquid mixture, *Phys. Rev. E - Stat. Physics, Plasmas, Fluids, Relat. Interdiscip. Top.* 69 (2004) 6. <https://doi.org/10.1103/PhysRevE.69.011402>.
- [53] S.L. Hager, T.B. Macrury, Investigation of phase behavior and water binding in poly(alkylene oxide) solutions, *J. Appl. Polym. Sci.* 25 (1980) 1559–1571.
<https://doi.org/10.1002/app.1980.070250805>.